

Expansion of Confined Disposal Facilities

APPENDIX F1
COASTAL DESIGN APPENDIX

TABLE OF CONTENTS

Paragraph	Title	Page
1	Introduction	1
2	Existing CDFs	1
3	Subsurface Information	1
3.1	Existing Subsurface Information	1
3.2	Subsurface Information Needed for Detailed Design	2
4	Lake Levels	3
5	Wave Analysis	3
5.1	General	3
5.2	Deepwater Waves	3
5.3	Incident Waves: Goda Method	7
5.4	Incident Waves: TMA Method	11
5.5	Adopted Incident Waves	12
6	Dike Cross-section Design	13
6.1	General	13
6.2	Stone Sizes	13
6.3	Crest Height	14
6.4	Stability	15
6.5	Settlement	15
7	Dredge Material Consolidation	15
8	Plan Discussion	16
8.1	General	16
8.2	New CDF Adjacent to Cell 1	17
8.3	New CDF Adjacent to Island 18	17
9	References	18

TABLES

Number	Title	Page
1	Lake-Level-Frequency Information	3
2	Annual Maximum Wave Heights within Wave Directions 30 - 96 Degrees	5
3	Annual Maximum Wave Heights within Wave Directions 0 - 58 & 264 - 360 Degrees	6
4	Deepwater Wave Information	7
5	Refraction Coefficients and Unrefracted Deepwater Wave Heights	9
6	Determination of Incident Wave Height	9
7	Determination of Breaking Wave Conditions	10
8	Incident Significant Design Waves Computed Using TMA and Compared with The Goda Analysis	12
9	Adopted Design Waves	13
10	Calculated Stone Sizes	14
11	Required Capacity of New CDF	17

FIGURES

Number	Title	
1	West End of Lake Erie	13
2	Location of Existing CDFs	14
3	Typical Cross-section along Northern Side of Existing CDF, Cell 1	15
4	Typical Cross-section along Eastern Side of Existing CDF, Cell 1	15
5	Typical Lakeside Dike Cross-section, Cell 2	15
6	Deepwater Wave Angle Band: 30 to 96 Degrees	16
7	Deepwater Wave Angle Band: 264 to 58 Degrees	16
8	Deepwater Wave Height - Frequency Curve	17
9	Deepwater Wave Height - Frequency Curve	18
10	Wave Period as a Function of Wave Height	19
11	Wave Period as a Function of Wave Height	20
12	Typical Lakeside Dike Cross-section for Proposed CDF	20
13	Potential CDF Locations Identified in Final EIS Dated June 1990	21
14	Depths Contours Used to Calculate Volume of Proposed CDF Adjacent to Cell 1 for Varying Widths	22
15	Dredged Storage Capacity of Proposed CDF adjacent to Cell 1	23
16	Proposed CDF Adjacent to Cell 1, Alternative Size A	24
17	Proposed CDF Adjacent to Cell 1, Alternative B	25
18	Proposed CDF Adjacent to Cell 1, Alternative Size C	26
19	Depths Contours Used to Calculate Volume of Proposed CDF Adjacent to Island 18 for Varying Widths	27
20	Dredged Storage Capacity of proposed CDF Adjacent to Island 18	28
21	Proposed CDF Adjacent to Island 18, Alternative Size A	29
22	Proposed CDF Adjacent to Island 18, Alternative Size B	30
23	Proposed CDF Adjacent to Island 18, Alternative Size C	31

1 INTRODUCTION

Toledo Harbor is located at the western end of Lake Erie in Lucas County, Ohio. Authorization for harbor improvements first began with the River and Harbor Acts of 1899. The project provides for a channel 28 feet deep and 500 feet wide from deep water in Lake Erie to the mouth of the Maumee River, a distance of approximately 18 miles. The river channel then follows the Maumee River for approximately 7 miles upstream. In order to maintain the channel, approximately 850,000 cubic yards of river sediment is dredged annually. A portion of this material is dumped in the open-lake, with the remainder placed in existing Confined Disposal Facilities (CDFs). As restrictions increase in open-lake dumping, a higher percentage will be required to be placed into CDFs. This report will identify potential sites for a new CDF. Three sizes will be investigated, with the variation resulting from the assumed amount of open-lake disposal allowed. *Figure 1* presents the location of Toledo Harbor at the western end of Lake Erie.

2 EXISTING CDFs

Dredged sediment from Toledo Harbor is presently placed in the authorized open-lake disposal area and the existing CDFs. Presently there are three US Army Corps of Engineers' CDFs: Island 18, Cell 1 and Cell 2. The newest CDFs are Cell 1 and Cell 2. Cell 1 was completed in 1976 and Cell 2 was completed in 1993. The crest elevation for these CDFs are at 23.5 feet above Low Water Datum (LWD). *Figure 2* presents the location of the aforementioned CDFs. *Figure 3* and *4* present typical cross-sections of the Cell 1 dike and *Figure 5* presents a typical cross-section of the Cell 2 dike.

3 SUBSURFACE INFORMATION

3.1 Existing Subsurface Information

Existing subsurface information consists of borings drilled for the design of the adjacent Cell No.1 and Cell No.2 dike disposal facilities.

In July 1972, Buffalo District had eight drive sample borings drilled into the lake bottom at the location of Cell No.1. These borings were drilled to depths of 28.7 to 54 feet below low water datum (El. 568.6 I.G.L.D.). Results of these explorations revealed that the upper 1 to 4 feet consisted of very soft organic silt and clay. Underneath the very soft deposits is 11 to 22 feet of medium silty clay overlying very stiff to hard silty clay. No bedrock was encountered in any of the borings.

In September and October 1986, Buffalo District had 11 drive sample borings and five undisturbed sample borings drilled into the lake bottom at the location of Cell No.2. The drive sample borings were obtained by employing standard penetration resistance methods (2 inch O.D. split spoon sampler driven by 140 lb hammer falling from 30 inch drop). The undisturbed samples were obtained by employing 5 inch diameter Shelby Tubes. Due to unfavorable conditions encountered by the drive sample and undisturbed sample borings, six additional probe borings were performed to delineate the soft soil deposits. The probes employed an AW drilling rod which was driven by a 140 lb hammer falling from a height of 30 inches. The blow counts required to drive the probe rod each six inches were recorded on a log form.

Results of these explorations revealed that the consistency of underlying lake bottom soil deposits varied considerably from location to location. Alluvial deposits consisting of soft silty and sandy clays make up the top 5 to 7 feet and overly stiff glacial till consisting of silty and sandy clay. In a number of borings, however, a very soft organic silt deposit was encountered which varied in thickness from several feet to as much as 15 feet.

3.2 Subsurface Explorations Needed For Detailed Design

Prior to the start of detailed design, subsurface explorations would be performed to determine the extent and thickness of any soft foundation deposits. The types of explorations to be performed are between 5 to 8 drive sample borings and 3 to 5 undisturbed sample borings. The drive sample borings would be obtained by employing standard penetration methods (drive 2" O.D. split sampler with 140 lb hammer falling from a height of 30 inches) and recording the penetration resistance for every 6 inches of sampler advance. This would provide general information on the consistency of the lake bottom foundation soils and would provide empirical information with respect to foundation shear strengths. The undisturbed samples would employ a 5 inch O.D. Shelby tube. The undisturbed samples would then be sent to a lab for laboratory shear strength and consolidation testing.

4 LAKE LEVELS

The National Oceanic and Atmospheric Administration (NOAA) has operated a lake elevation recording gage at Toledo, OH since 1941. The 10-year and 20-year lake levels are presented in *Table 1* (USAED Detroit, 1993).

Table 1. Lake Level-Frequency Information

Recurrence Interval	Water Level	
	IGLD (1955)	LWD
10-year	576.43	7.8
20-year	576.75	8.1

5 WAVE ANALYSIS

5.1 General

This section presents the summary of the deepwater waves and the methodology to obtain the incident waves at the proposed structures. Incident waves were determined using two algorithms: the method of Goda and the TMA method. The design wave was selected based upon the results of these analyses.

5.2 Deepwater Waves

A wave hindcast was recently developed for 53 stations along the Lake Erie shore based upon thirty-two years (1956-1987) of meteorological data (Driver, et. al., 1991). The nearest wave hindcast station to Toledo Harbor is WIS Station 01 at 83.27W and 41.73N. Significant wave height-recurrence interval information was developed for three class angles. However, corresponding wave period-frequency information is unavailable. Since significant deepwater wave heights, peak period and direction are also available at 3 hour intervals, this data was used to develop the deepwater wave height and period- frequency relationships.

In order to obtain the deepwater wave height- frequency relation, the entire 32-year data set was imported into a spreadsheet program. The largest wave for each year during the navigation season for the period of record (1956 - 1987) was ranked and the associated recurrence interval determined using the Weibull formula:

$$RI = N+1/M$$

where RI = recurrence interval in years

N = number of years of record (32)

M = rank (highest = 1)

Based upon the potential location of the new CDFs, two wave angle bands were selected. It is anticipated that these directions would be the most representative of waves approaching the proposed structures. Wave angle bands of 300(N30E) to 960(S84E), and 2640(S84W) to 580(N58E), which would affect the northern side and eastern side of the proposed CDFs, respectively, were considered and are shown on *Figures 6* and *7*. *Tables 2* and *3* present the maximum annual deepwater wave heights for the period of record and their respective recurrence interval for the two wave angle bands. *Figure 8* and *9* present the resulting deepwater wave height - frequency curves for the two wave angle bands.

TABLE 2. Annual Maximum Wave Heights within Wave Directions 30 - 96 Degrees

Year	Date	Hour	Wave Height in Feet	Wave Period in Seconds	Azimuth in Degrees	Rank	Probability in Percent
1957	4-APR	1200	7.2	8.3	90	1	3.03
1975	18-OCT	1200	7.2	8.3	43	2	6.06
1982	6-APR	600	7.2	6.7	43	3	9.09
1984	28-FEB	300	7.2	6.7	56	4	12.12
1964	12-JAN	2100	6.9	5.9	53	5	15.15
1972	7-APR	1800	6.9	8.3	51	6	18.18
1986	7-FEB	600	6.9	7.1	69	7	21.21
1962	7-MAR	0	6.6	9.1	51	8	24.24
1966	27-APR	1800	6.6	7.1	80	9	27.27
1968	13-MAR	0	6.6	8.3	46	10	30.30
1978	4-MAY	1800	6.6	7.1	73	11	33.33
1979	26-FEB	600	6.6	8.3	56	12	36.36
1961	13-APR	300	6.2	7.7	53	13	39.39
1965	16-JAN	1800	6.2	7.7	51	14	42.42
1969	19-APR	300	6.2	8.3	51	15	45.45
1974	8-APR	2100	6.2	8.3	45	16	48.48
1977	5-DEC	1800	6.2	6.7	56	17	51.52
1980	14-APR	1500	6.2	7.1	70	18	54.55
1985	28-NOV	900	6.2	7.1	56	19	57.58
1987	24-APR	2100	6.2	7.7	45	20	60.61
1958	27-FEB	1800	5.9	6.7	91	21	63.64
1959	27-MAR	0	5.9	6.2	76	22	66.67
1970	29-MAR	1800	5.9	6.7	54	23	69.70
1976	25-APR	1800	5.9	6.2	56	24	72.73
1983	9-APR	1800	5.9	5.9	75	25	75.76
1960	12-DEC	600	5.6	7.7	46	26	78.79
1967	10-DEC	1800	5.6	6	7 87	27	81.82
1971	7-APR	0	5.6	7	7 50	28	84.85
1973	27-MAR	0	5.6	7.7	45	29	87.88
1963	13-SEPT	1500	5.2	7.1	53	30	90.91
1956	28-MAR	300	4.9	5.6	72	31	93.94
1981	1-DEC	600	4.9	5.6	92	32	96.97

**TABLE 3. Annual Maximum Wave Heights within Wave Directions
0 - 58 & 264 -360 Degrees**

Year	Date	Hour	Wave Height in Feet	Wave Period in Seconds	Azimuth in Degrees	Rank	Probability in Percent
1982	6-Apr	900	7.2	9.1	21	1	3.03
1975	18-Oct	900	7.2	8.3	57	2	6.06
1984	28-Feb	300	7.2	6.7	56	3	9.09
1972	7-Apr	1800	6.9	8.3	51	4	12.12
1964	12-Jan	2100	6.9	5.9	53	5	15.15
1962	7-Mar	0	6.6	9.1	51	6	18.18
1968	3-Mar	0	6.6	8.3	46	7	21.21
1979	26-Feb	600	6.6	8.3	56	8	24.24
1969	19-Apr	300	6.2	8.3	51	9	27.27
1974	8-Apr	2100	6.2	8.3	45	10	30.30
1961	13-Apr	300	6.2	7.7	53	11	33.33
1965	16-Jan	1800	6.2	7.7	51	12	36.36
1983	24-Apr	1800	6.2	7.7	27	13	39.39
1987	24-Apr	2100	6.2	7.7	45	14	42.42
1985	28-Nov	900	6.2	7.1	56	15	45.45
1977	5-Dec	1800	6.2	6.7	56	16	48.48
1959	27-Mar	2100	6.2	6.2	25	17	51.52
1978	20-Jan	1800	5.9	8.3	53	18	54.55
1970	29-Mar	2100	5.9	7.7	58	19	57.58
1976	25-Apr	1800	5.9	6.2	56	20	60.61
1957	8-Apr	2100	5.6	7.7	27	21	63.64
1960	12-Dec	600	5.6	7.7	46	22	66.67
1971	7-Apr	0	5.6	7.7	50	23	69.70
1973	27-Mar	0	5.6	7.7	45	24	72.73
1966	13-Apr	0	5.6	5.9	56	25	75.76
1967	7-May	1800	5.6	5.3	25	26	78.79
1958	26-Mar	600	5.2	7.7	50	27	81.82
1963	13-Sep	1500	5.2	7.1	53	28	84.85
1986	7-Feb	1500	4.9	5.9	32	29	87.88
1980	26-Feb	300	4.9	5.6	23	30	90.91
1956	16-Mar	1500	4.9	5.3	52	31	93.94
1981	6-May	2100	4.6	5.3	44	32	96.97

The wave period for the corresponding deepwater wave height was plotted for both angle bands on *Figures 10 and 11*. As can be seen from these figures, there is a wide variation in peak wave period for any given wave height. For design purposes, the largest wave period for a selected wave height will be used.

Table 4 presents the deepwater wave heights and periods used for the design of the proposed CDFs at Toledo Harbor.

Table 4. Deepwater Wave Information

Recurrence Interval	Structure Leg (Orientation)	Deepwater Wave Height, H_0 , in Feet	Peak Wave Period, T_p , in Seconds
10-year	North	7.0	9.1
	East&South	7.1	9.1
20-year	North	7.2	9.1
	East&South	7.3	9.1

5.3 Incident Waves: Goda Method

Incident waves along the northern and eastern legs of the proposed CDFs were determined for the combination of the 20-year lake level and 10-year all-season wave as well as the 10-year lake level and 20-year all-season wave.

Waves are irregular in height, period and direction. The methodology to compute the transformation and attenuation of irregular waves propagating from deep water based upon work done by Goda has been summarized in Seelig and Ahrens (1980) and is intended for open sections of the coast with continuously shallowing depth contours. Design curves were developed to compute refraction coefficients and nearshore wave breaking. Refraction calculations are based on the energy-weighted superposition of refraction coefficients obtained from linear theory and include directional spreading of wave energy. The method is intended for the case of straight parallel bottom contours. Calculation of refraction coefficients, K_R , and nearshore wave direction angle, α , using the design curves in Seelig and Ahrens (1980) require the dominant deepwater wave direction angle, α , an estimate of the variation of energy level with wave direction parameter, S^* , and the peak wave period, T_p . The recommended value for S^* is 4.0 (wind waves). The estimation of the refraction coefficient allows the calculation of the equivalent deepwater wave height, H_0' , which is determined from

$$H_0' = K_R H_0$$

where H_0 (also labelled as H_{m0} in this report) is defined as the deepwater significant wave height.

The nearshore wave height prediction model for irregular waves accounts for wave breaking, nonlinear wave shoaling, irregular wave setup and surf beat. Goda's approach allows broken waves to reform at a lower height. The significant wave height at the structure, H_{sig} , and the one-percent wave height, H_1 , were calculated using H_0' , T_p , the offshore bottom slope, m , and the water depth, d . Since the design waves did not vary significantly for the orientation, the largest waves presented in *Table 4* were used. *Tables 5 and 6* present the incident wave analysis and *Table 7* presents the breaking wave analysis for waves incident to the proposed Plan 1.

Table 5. Refraction Coefficients and Unrefracted Deepwater Wave Height

Design Water Level	Design Wave	α_0 degrees	T_p Seconds	d Feet	d/gT_p^2	K_r	H_0 Feet	H_0' Feet
10-YR (+7.8 ft LWD)	20-YR	0	9.1	13.8	0.0052	.91	7.3	6.6
20-Yr (+8.1 ft LWD)	10-YR	0	9.1	14.1	0.0053	.91	7.1	6.5

Table 6. Determination of Incident Wave Height

Design Water Level	Design Wave	H_0' Feet	d Feet	L_0 Feet	$\frac{H_0'}{L_0}$	d/H_0'	$\frac{H_{sig}}{H_0'}$	H_{sig} Feet	$\frac{H_1}{H_0'}$	H_1 Feet
10-YR (+7.8 ft LWD)	20-YR	6.6	13.8	422.3	0.016	2.09	1.15	7.6	1.56	10.3
20-Yr (+8.1 ft LWD)	10-YR	6.5	14.1	422.3	0.015	2.17	1.17	7.6	1.60	10.4

Table 7. Determination of Breaking Wave Conditions

Case	H_0' Ft	T_p sec	$\frac{H_0'}{gT_p^2}$	S	$\frac{H_b}{H_0'}$ (1)	H_b Feet	$\frac{H_b}{gT_p^2}$	$\frac{d_b}{H_{bmin}}$ (2)	$\frac{d_b}{H_{bmax}}$ (2)	d_{bmin} Feet	d_{bmax} Feet	d Feet	Wave Type
10-YR Water Level & 20-YR Wave	6.6	9.1	.0025	.01	1.54	10.2	.0038	1.2	1.52	12.2	15.5	13.8	BRK
20-YR Water Level & 10-YR Wave	6.5	9.1	.0024	.01	1.54	10.0	.0038	1.2	1.52	12.0	15.2	14.1	BRK

- (1) From SPM (1984) Figure 7-3.
- (2) From SPM (1984) Figure 7-2.
- (3) "BRK" means breaking wave.

5.4. Incident Waves: TMA Method

Waves at the proposed structures were also determined via application of a shallow-water self-similar spectral form (Hughes, 1984). Self-similarity in spectral form implies that there is a relative balance between wind energy input, energy transfers within the spectrum, and energy dissipation. This balance is maintained and limited to produce a consistent spectral shape. This spectral form, referred to as the TMA spectrum, substitutes an expression for the shallow-water equilibrium range into the JONSWAP equation for spectral energy density. The JONSWAP parameters are empirically defined through examination of over 2,800 wind sea spectra obtained at various depths and locations. This spectral form is intended to describe single-peaked wind seas which have reached a growth equilibrium in finite depth water.

The primary underlying assumption is that the wind sea is at a steady state condition. This means that the wind has been steady long enough for the waves to reach equilibrium and that the bottom topography is a gentle slope with smoothly varying features and without complexities which might cause rapid alteration of the wave train. Generally a maximum slope of 1V:100H is suggested. The TMA spectrum as it is presently parameterized can not be used in fetch- or duration-limited shallow-water wave growth situations since it is a final steady state form.

The TMA equations require specification of the wind speed, U, the water depth, d, and the peak deepwater wave frequency, f_p . When wave conditions are steady and the combination of beach slope and propagation distance are sufficiently small, negligible shift in the peak wave frequency occurs from deepwater into shallow water.

The solution of the following series of equations is required:

Step 1. Determine the dimensionless wave number, κ ,

$$\kappa = U^2 2\pi (gL_m)$$

Step 2. Determine the spectral parameter, α ,

$$\alpha = 0.0078 \kappa^{0.49}$$

Step 3. Select proper equation for the zero-moment wave height, H_{mo} , by determining the wave frequency where $\omega_d=1$, i.e.,

$$\omega_d = 2\pi f' (d/g)^{1/2} = 1$$

or

$$f' = (g/d)^{1/2} / 2\pi$$

For peak frequencies greater than $1.5f'$ (peak periods less than $1.5T'$), the wavelength should be determined using the intermediate depth linear dispersion relation and H_{mo} determined using the first equation in step 4. Otherwise the second equation for shallow water conditions should be used.

Step 4. The depth-limited significant wave height equation is selected from:

$$H_{mo} = (1/\pi)\alpha^{1/2}L_m$$

or taking $L_m = (gd)^{1/2}T_p$ in shallow water gives

$$H_{mo} = (1/\pi)(\alpha gd)^{1/2}T_p$$

Step 5. Determine the significant wave height, H_s , defined as the average of one-third of the highest waves. This computation is accomplished because H_s is more representative than H_{mo} of actual crest-to-trough wave heights and should be used in those applications (such as structure design) where the effect of individual waves is more important than the average wave energy. Figure 1 in CETN-I-45 (USAEWES,1991) presents the variation of H_s/H_{mo} as a function of the relative d and significant steepness.

The above series of equations were solved for a 20-year depth of 14.1 feet, a peak wave period of 9.1 seconds and a varying wind speed. For a 40- and 50-mph wind, significant wave heights of 7.0 and 7.8 feet were calculated, respectively.

5.5 Adopted Incident Waves

Table 8 compares the results of the wave obtained using Goda's algorithms with that using the TMA methodology. As can be seen from this table, similar results were obtained using both methods.

Table 8. Incident Significant Design Waves Computed using TMA and Compared with the Goda Analysis

METHOD	U - wind speed	H_s
Goda	—	7.6 feet
TMA	40 mph	7.0 feet
TMA	50 mph	7.8 feet

Hence, the selected design waves developed using Goda's methodology will be adopted. The design waves used for the structure design are presented in *Table 9*.

Table 9. Adopted Design Waves

Variable	Value
H_s	7.6 feet
H_1	10.4 feet
T_p	9.1 seconds

6 DIKE CROSS-SECTION DESIGN

A6.1 General - One typical cross-section shall be designed and will be considered applicable to the proposed CDFs. The typical section developed for Cell 2 will be used, with appropriate modifications made to the protective outer stone cover based upon the adopted design wave. The following subparagraphs summarize the design parameters. These findings were used to develop the typical cross-section presented on *Figure 12*.

6.2 Stone Sizes

Individual armor stone weights were determined using Hudson's formula (SPM, 1977):

$$W = \frac{W_r H^3}{K_D (S_r - 1)^3 \text{Cot}\theta}$$

where: W = weight of armor unit in primary cover layer

W_r = unit weight of armor

H = design wave height

K_D = stability coefficient

S_r = specific gravity of the armor unit

$\text{Cot}\theta$ = structure inverse slope

A rubblemound structure is composed of various sized layers designed to effectively dissipate wave action and prevent the migration of stone between each layer. The adopted gradation for rough angular stone is as follows:

Armor: 0.9W to 2.0W

Underlayer: 0.06W to 0.2W

Bedding: 0.00015W to 0.01W

No further gradation requirements are imposed upon the quarry. However, during plans and specifications, it should be ascertained if a standard product is available from local quarries which would meet the required range of size for the stone. The thickness of the layer is computed using (SPM, 1984):

$$r = nk_{\Delta} (W/W_r)^{1/3}$$

where: r = layer thickness

n = number of units comprising the layer

k_{Δ} = layer coefficient

$$= 1.0$$

W = Armor weight. An average weight of the gradation is used.

Stone weights and layer thicknesses were calculated for the typical section using the above equations. For all computations, a unit weight of the stone of 165 pounds/cuft was used. The stability coefficient varies with the type of incident wave (breaking/nonbreaking), the structure side slope and function (head or trunk). A stability coefficient ($K_D=3.5$) for breaking waves, structure trunk and 1V:2H side slope was adopted. The calculated stone size summary is presented in *Table 10*.

Table 10. Calculated Stone Sizes

K_D (1)	Armor		Underlayer	
	Size LBS	2-layer Thickness FT	Size LBS	2-Layer FT
3.5	2100 - 4600	5.5	900 - 310	2.0

(1) Structure side slope at 1V:2H.

6.3 Crest Height

The stone armor protection along the lakeside of the proposed dikes should extend up to the limit of wave runup from the one-percent waves, H_1 . The wave runup on a rough sloped structure is estimated using Ahrens and McCartney (1975):

$$R = H_1[a \xi(1+b \xi)]$$

where $a = 0.775$ (USAEWES,1992)

= surf similarity parameter

$$= \tan\theta(H_1/L_0)^{0.5}$$

θ = angle of lakeward face of breakwater

L_0 = deepwater wavelength

$b = 0.361$ (USAEWES,1992)

The values for a and b are valid for a rubblemound structure with an impermeable core as will be the proposed dike structures. The resulting wave runup of 11.9 feet superimposed on a 20-year water level of +8.1 ft LWD, results in the limit of wave runup of +20.0 feet LWD. This elevation shall be selected as the crest of the stone protection.

6.4 Stability

The proposed dike design cross section is similar to the dike cross section for Cell No.2 with the exception that the lakeside armor stone face is to extend to +20' LWD as opposed to +14' LWD. The foundation conditions and material properties (i.e. shear strength, unit weight) for the new CDF is expected to be similar to Cell No.1 and Cell No.2. Therefore, the proposed new CDF dike design cross section should be stable.

6.5 Settlement

As discussed above, the foundation conditions and material properties for the new CDF is expected to be similar to Cell No.1 and Cell No.2. The design analysis for Cell No.2 estimated that the total ultimate (long term) settlement of the containment dike

centerline to be on the order of about 2.5 feet. As the new disposal facility is being filled, both the containment dike and placed dredged material spoil will both undergo settlement. To insure that the dredged spoil will not overtop the containment dike, a 2.5 foot freeboard between the dredged spoil and dike crest has been incorporated into the design.

7 DREDGE MATERIAL CONSOLIDATION

In order to size the new CDF, a dredge material consolidation factor was determined based upon computer model results and actual filling rates for Cell No.1. The dredge material consolidation factor is the percentage of the total dredged insitu volume remaining after the dredged material has been consolidated over a specified time period. In developing this factor, the dredged material undergoes four processes: (1.) Bulking (after material is dredged), (2.) Settling (immediately after dredged material is placed in CDF), (3.) Dessication and drying, (4.) Consolidation (Self weight consolidation and consolidation due to imposed loads from subsequent dredged fill layers).

Using dredge consolidation model INCPPDF90, historical dredging volumes and, surveys of Cell No.1, the dredge consolidation factor was determined. Over a 20 year period (1976 - 1996) the total volume of insitu dredged material placed in Cell No.1 was 12,625,902 cubic yards. At the end of the 20 year disposal period (1996) the computer model predicts that the dredge material would occupy 9,588,179 cubic yards in Cell No.1 assuming 100% drainage efficiency (well managed site with surface trenching). Thus, the volume reduction would be 24% calculated as follows:

$$(1 - (9,588,179 \text{cy} / 12,625,902 \text{cy})) \times 100 = 24\%$$

Based upon surveys of Cell No.1 in September 1996 the actual volume that the dredge spoil occupied is 9,521,878 cubic yards. This results in a corresponding volume reduction of 24.6% and closely matches that determined by the computer model.

Assuming a volume reduction factor of 24%, the consolidation factor used in the present analysis is .76 (1 - .24).

8 PLAN DISCUSSION

8.1 General

During the selection of the site for a new CDF in 1990 (USAED Buffalo, 1990), seven different alternative possibilities were considered as illustrated on *Figure 13*. Alternative 4, construction of a completely unattached, island-like CDF, was eliminated from detailed evaluation due to its extremely high costs and adverse aquatic effects. Alternative 4 would cover some of the old sidecast gravel bars that provide important spawning and feeding areas to fish species common to Maumee Bay. In addition, construction at Site 4 could have adverse effects on water quality in the bay by interfering with current mixing patterns. For similar reasons, Alternative 3A and 3B were also eliminated from detailed consideration. Alternative 2 would involve construction of three new dike walls about 15,000 feet in length, adjacent to the lakeward side of the existing Federal CDF (Cell 1). In addition to extremely high costs, this alternative was eliminated from detailed consideration due to its probable adverse effects on gravel bars on water circulation in the bay. Three different alternatives with varying dike heights were developed for Site 1. This site became the selected site and resulted in the construction of Cell 2.

For this investigation the site adjacent to Cell 1 and Island 18 will be studied. The required size of the proposed CDFs will be determined based upon three annual dredging amounts, which allow for no or partial open-lake disposal. The capacity (volume) needed in the new CDF is equal to the annual confined dredging quantity multiplied by the service life times the consolidation factor. *Table 11* presents the required capacity of the new CDF for the three annual confined dredging amounts assuming a 20-year service life.

Table 11. Required Capacity of New CDF

Dredging Alternative Size	Annual Confined Disposal Amount CY	20-Year Dredging Quantity CY	Consolidation factor	Capacity Needed in New CDF - CY
A	850,000	17,000,000	0.76	12,920,000
B	600,000	12,000,000	0.76	9,120,000
C	350,000	7,000,000	0.76	5,320,000

8.2 New CDF Adjacent to Cell 1

This proposed CDF would be located adjacent to existing Cell 1. It would share the east side of Cell 1, which has a length of 3695 feet. The required widths of the proposed cells were determined by developing a relationship for the cell capacity as a function of cell width. Depth contours were developed using the Thiessen method (Viessman, et al. 1972) with the capacity determined for a width of 1000-, 3000- and 5000-feet as shown on *Figure 14*. Based upon the resulting capacity-width relationship presented on *Figure 15*, the required width for the proposed CDF would be 3500-, 2500- and 1500- feet in order to accommodate 850,000-, 600,000- and 350,000-cubic yards annually for 20-years, respectively. *Figures 16 through 18* present the three proposed CDFs adjacent to Cell 1 for the three alternative sizes.

8.3 New CDF Adjacent to Island 18

This proposed CDF would be located adjacent to Island 18. As indicated in paragraph A8.1, two options were treated in a cursory manner in USAED (1990). One reason this site was not selected was due to structures covering some of the old sidecast gravel bars that provide important spawning and feeding areas to fish species common to Maumee Bay. An option was entertained for this report that would create a long, narrow CDF adjacent to the east side of Island 18. Using a width of approximately 1200-feet, the CDF would lie between the navigation channel and the gravel bars. Preliminary capacity computations revealed that the CDF would be excessively long (about 4,900-, 8,400- and 12,000-feet long for dredging alternatives A, B and C, respectively). For this reason, this option was not pursued.

A similar result would occur if a CDF was constructed in a northern direction similar to the narrow width proposed in USAED (1990). Hence, a more economically efficient CDF was investigated which would utilize the east side of Island 18, but be square in shape. Partial covering of the gravel bars would result from this alternative, as well as the previously discussed alternative. During future investigations, mitigation measures may be required, which may include the removal and creation of a new bar at a different location or the creation of an environmentally enhanced CDF cross-section. This latter option might include the creation of a wider toe berm with pea gravel mixed in with the armor. As was done for the proposed CDF adjacent to Cell 1, the required widths of the proposed cells were determined by developing a relationship for the cell capacity as a function of cell width. Depth contours were developed using the Thiessen method (Viessman, et al. 1972) with the capacity determined for a width of 2000-, 3000- and 4000-feet as shown on *Figure 19*. Based upon the resulting capacity-width relationship presented on *Figure 20*, the required width for the proposed CDF would be 3650-, 3100- and 2350- feet in order to accommodate 850,000-, 600,000- and 350,000-cubic yards annually for 20-years, respectively. *Figures 21 through 22* present the three proposed CDFs adjacent to Cell 1 for the three alternative sizes.

REFERENCES

- Ahrens, J.P. and McCartney, B.L. 1975. "Wave Period Effects on the Stability of Riprap," Proceedings of Civil Engineering in the Oceans/III, American Society of Civil Engineers, pp.1019-1034.
- Driver, D.B., Reinhard, R.D. and Hubertz, J.M. 1991. Hindcast Wave Information For The Great Lakes: Lake Erie, WIS RPT 22, US Army Engineer Waterways Experiment Station, Vicksburg, MS.
- Hughes, S.A. 1984. *The TMA Shallow-water Spectrum Description and Applications*, Technical Report CERC-84-7, US Army Corps of Engineers Waterways Experiment Station, Vicksburg, MS.
- Seelig, W.M. and Ahrens, J.P. 1980. "Estimating Nearshore Conditions for Irregular Waves," Technical Paper No. 80-3, US Army Engineer Waterways Experiment Station, Vicksburg, MS.
- US Army Engineer District Buffalo. 1990. Final Environmental Impact Statement, Combined Disposal Facility, Toledo Harbor, Ohio.
- US Army Engineer District Detroit. 1993. Design Water Level Determination on the Great Lakes, Detroit, MI.
- US Army Engineer Waterways Experiment Station 1977. Shore Protection Manual, Vicksburg, MS.
- US Army Engineer Waterways Experiment Station 1984. Shore Protection Manual, Vicksburg, MS.
- US Army Engineer Waterways Experiment Station 1991. *Clarification of Wave Heights from Wave Information Studies (WIS)*, Coastal Engineering Technical Note (CETN) I-45, Vicksburg, MS.
- US Army Engineer Waterways Experiment Station, Coastal Engineering Research Center. September 1992. Automated Coastal Engineering System (ACES), Version 1.07, Vicksburg, MS.
- Viessman, W., Harbaugh, T.E. and Knapp, J.W. 1972. *Introduction to Hydrology*, Intext Educational Publishers, New York.

Figure 1. West End of Lake Erie

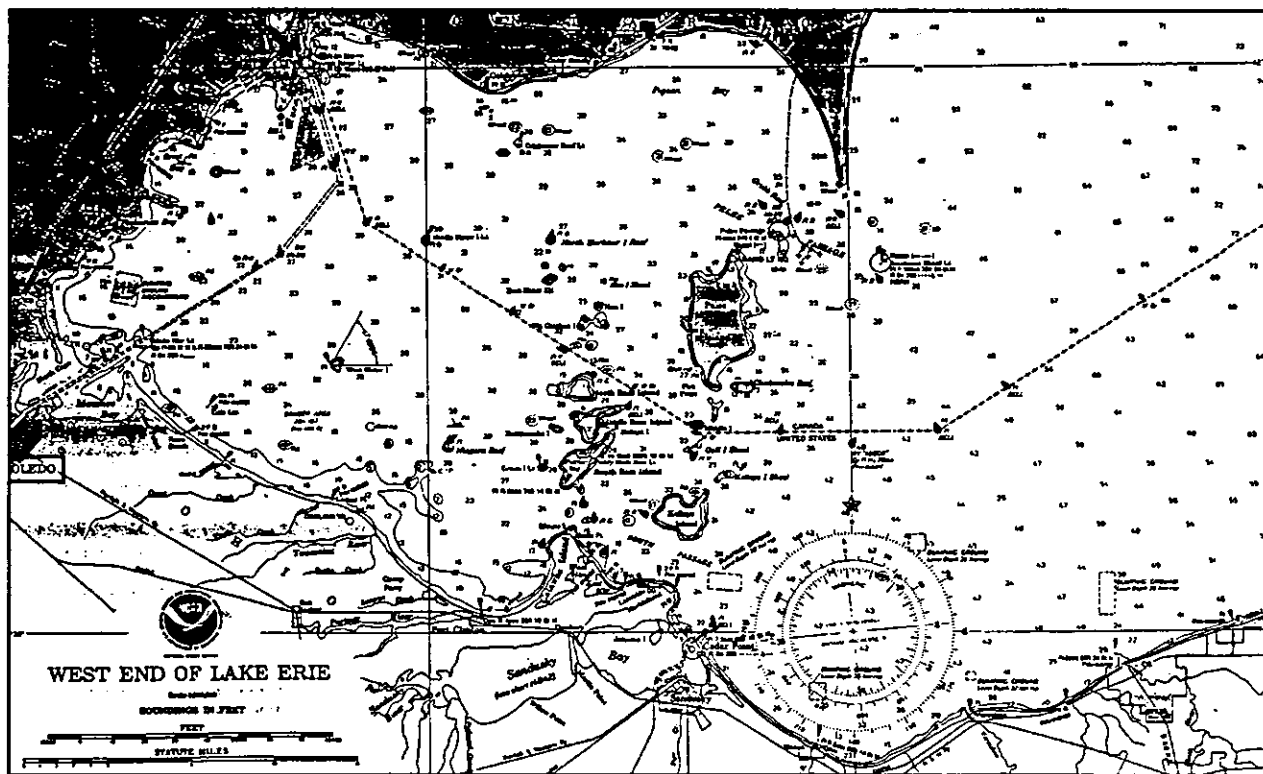


Figure 2. Location of Existing CDFs

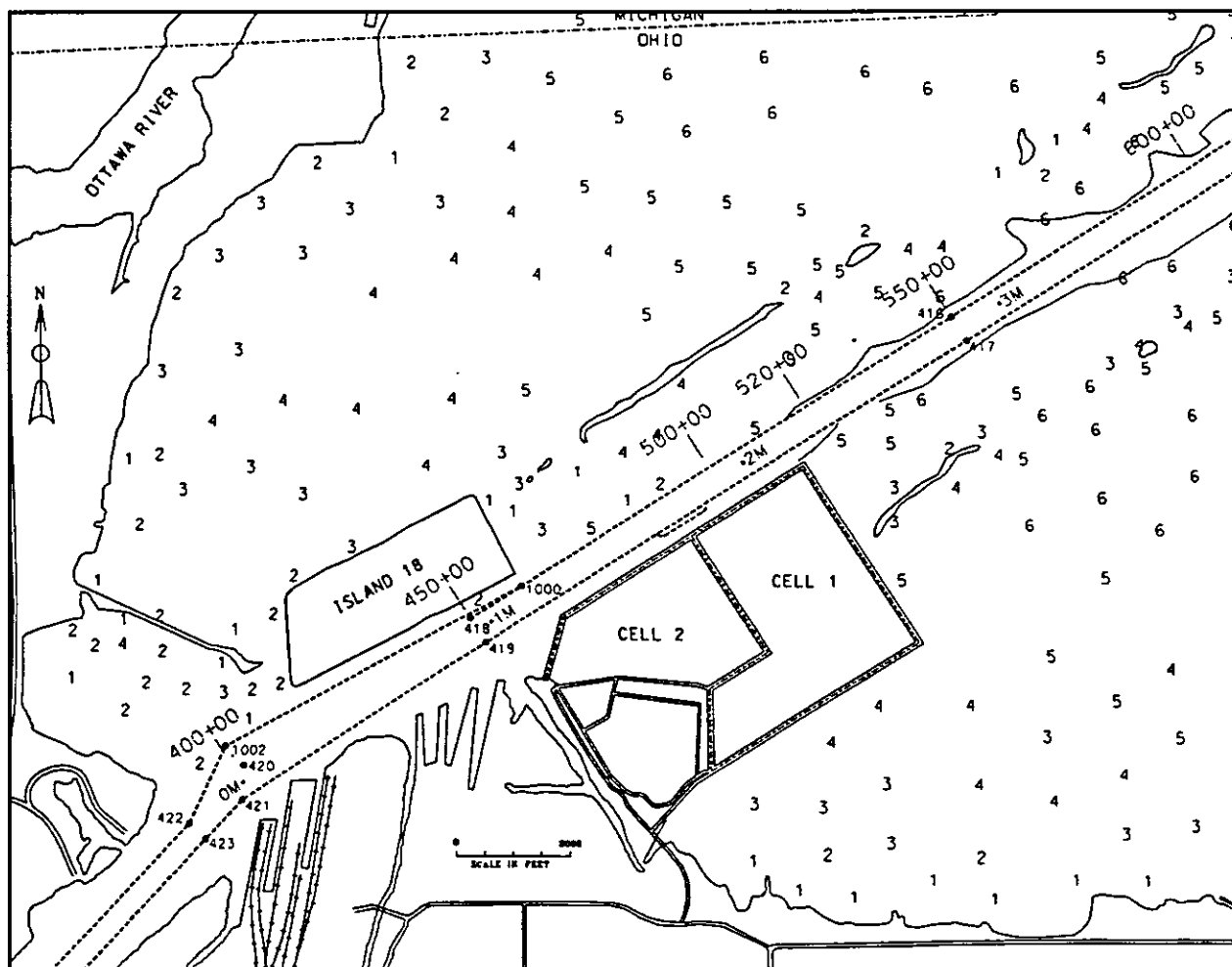


Figure 3. Typical Cross-Section Along Northern Side of Existing CDF, Cell 1

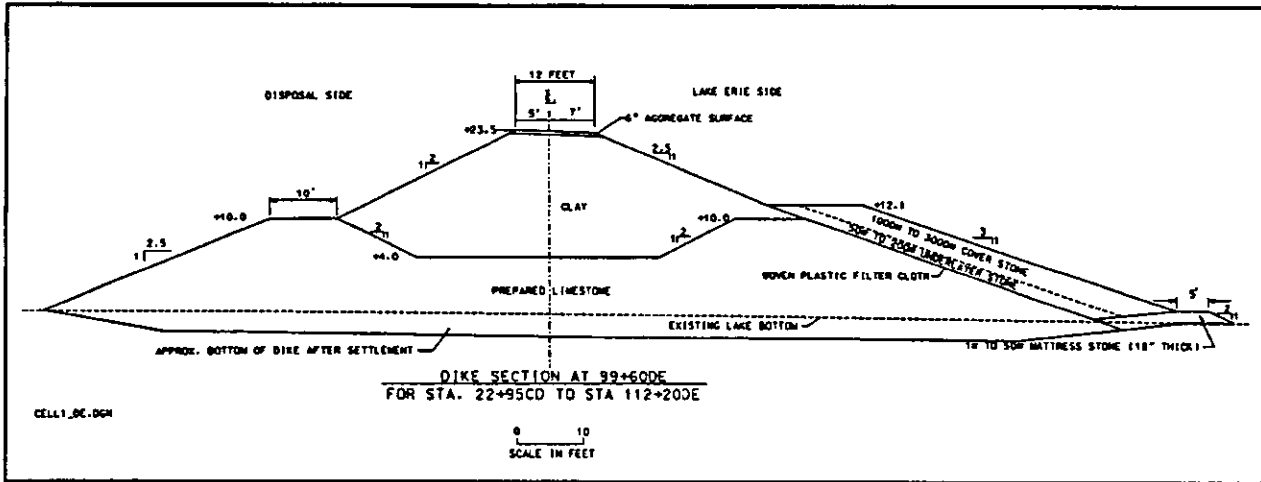


Figure 4. Typical Cross-Section Along Eastern Side of Existing CDF, Cell 1

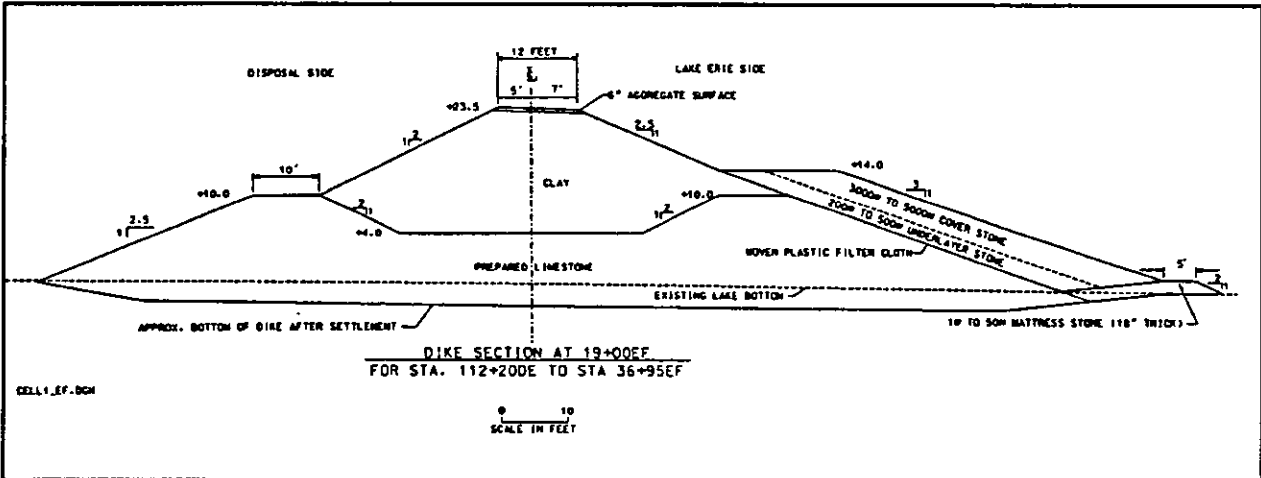


Figure 5. Typical Lakeside Dike Cross-Section, Cell 2

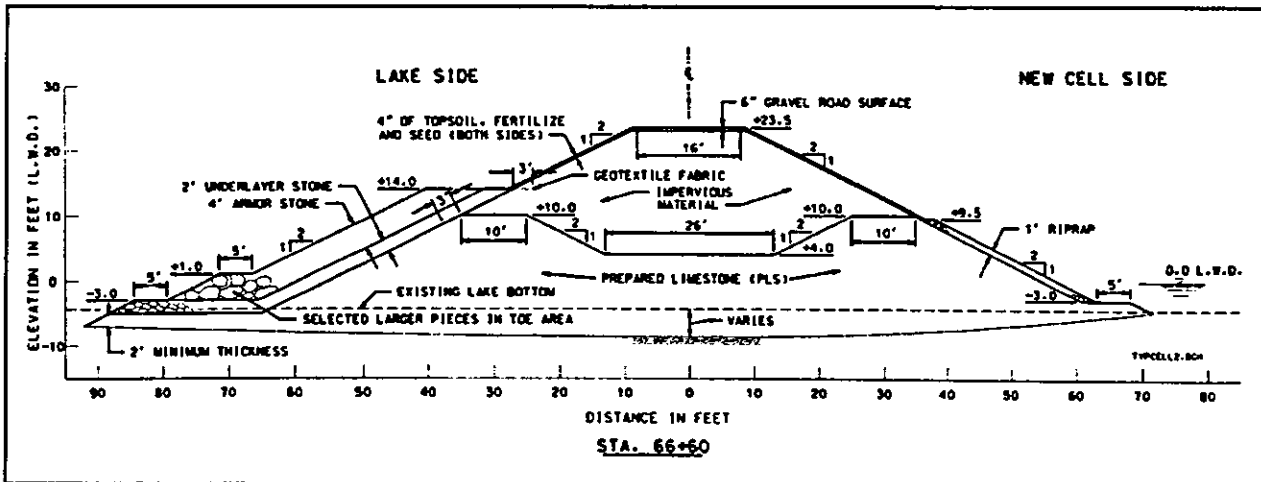


Figure 6. Deepwater Wave Angle Band: 30 to 96 Degrees

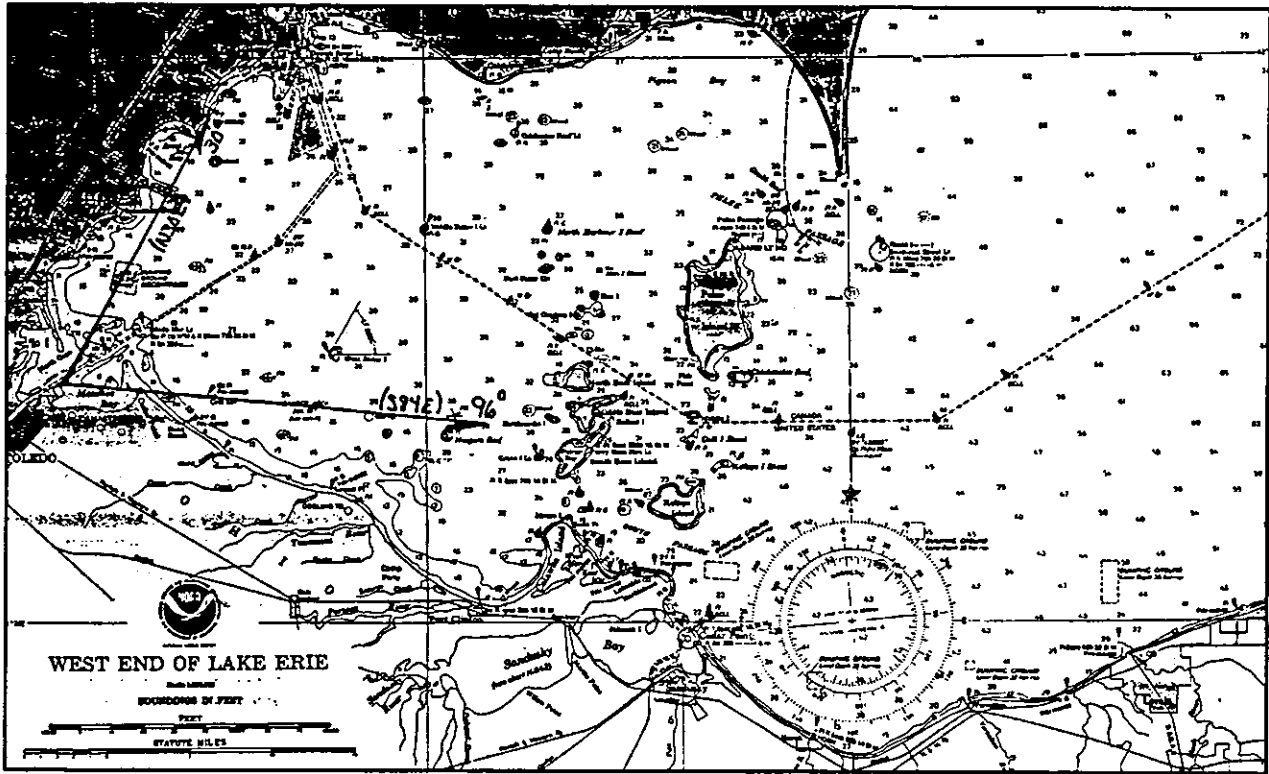


Figure 7. Deepwater Wave Angle Band: 264 to 58 Degrees

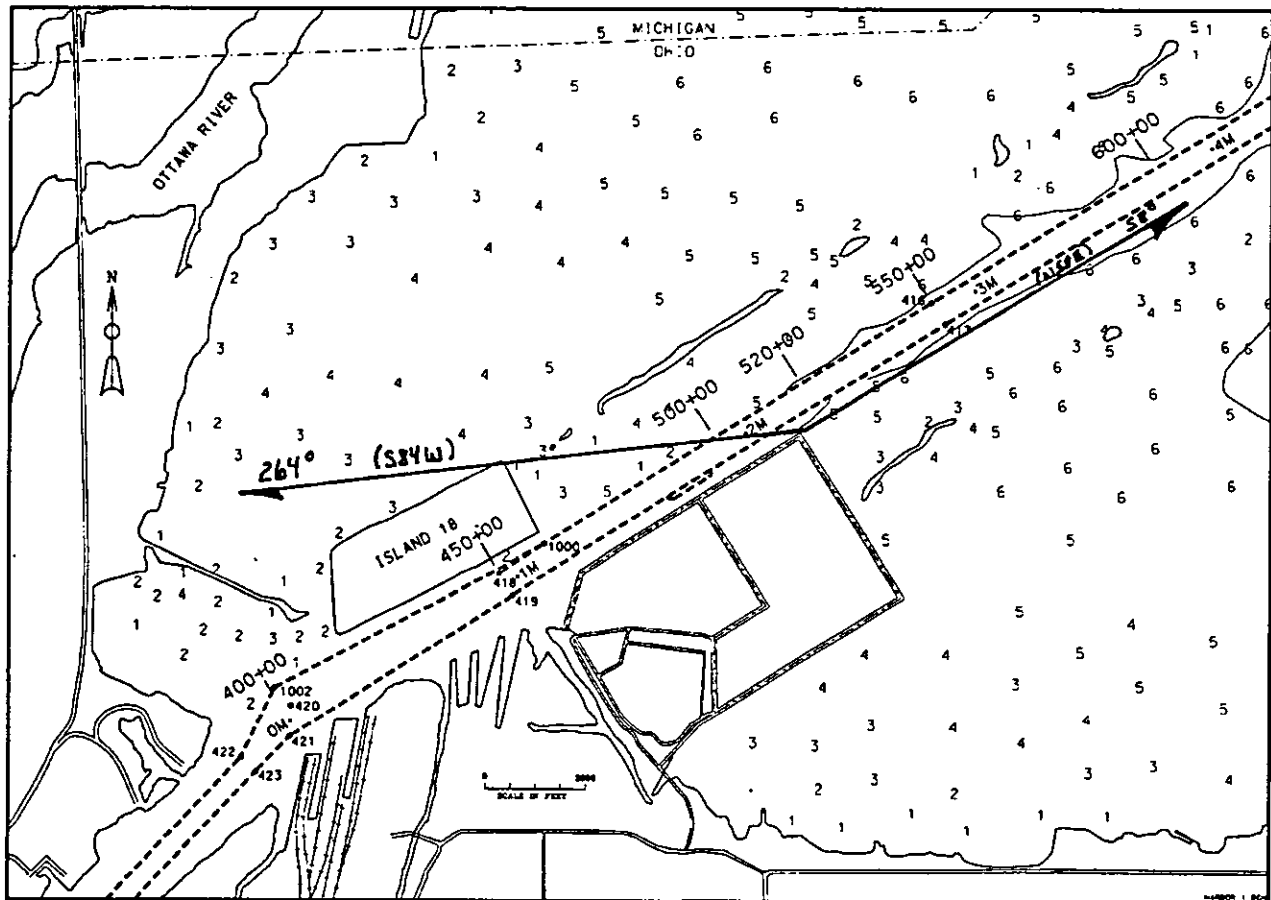


Figure 8. Deepwater Wave Height - Frequency Curve

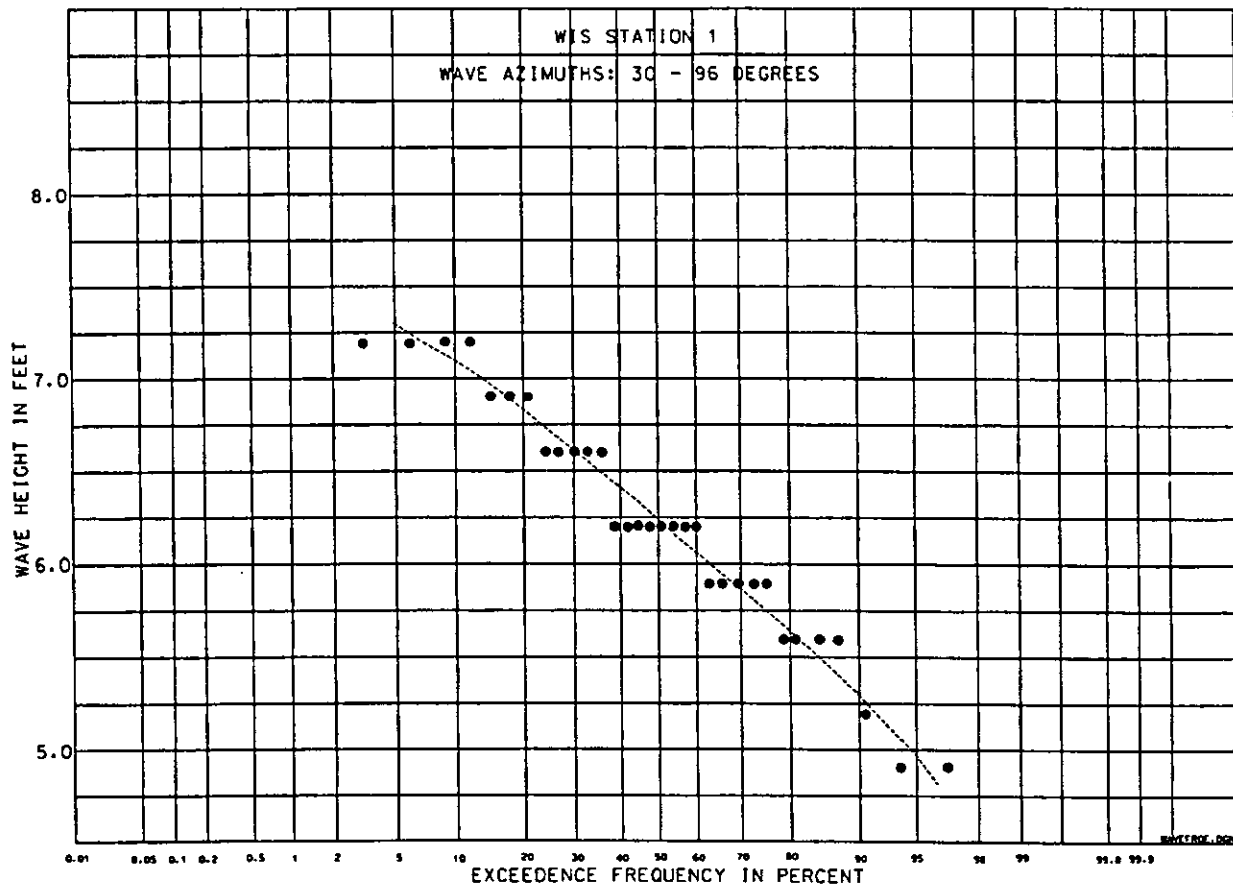


Figure 9. Deepwater Wave Height - Frequency Curve

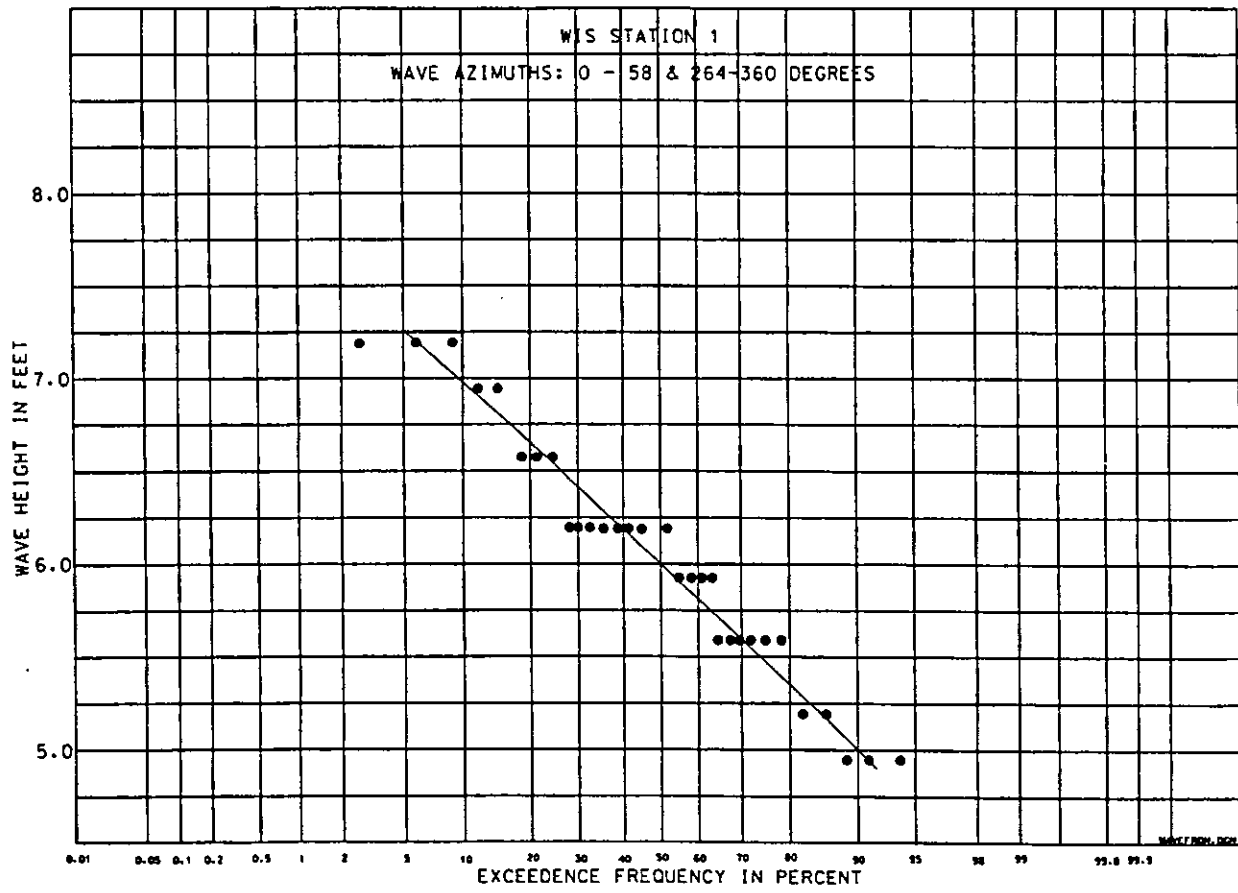


Figure 10. Wave Period as a Function of Wave Height

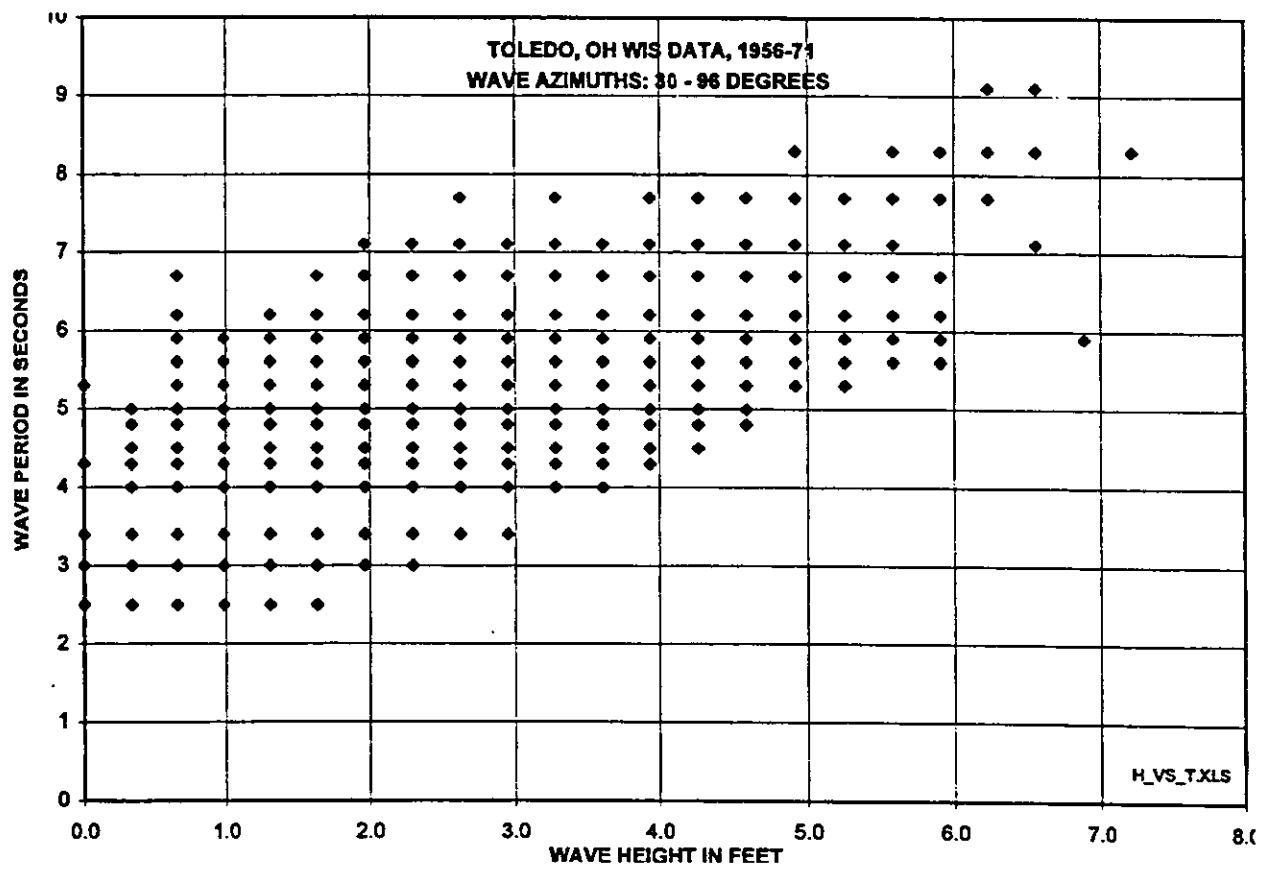


Figure 11. Wave Period as function of Wave Height

TOLEDO, OH WIS DATA, 1956-71
AZIMUTHS: 0-58 & 264-360 DEGREES

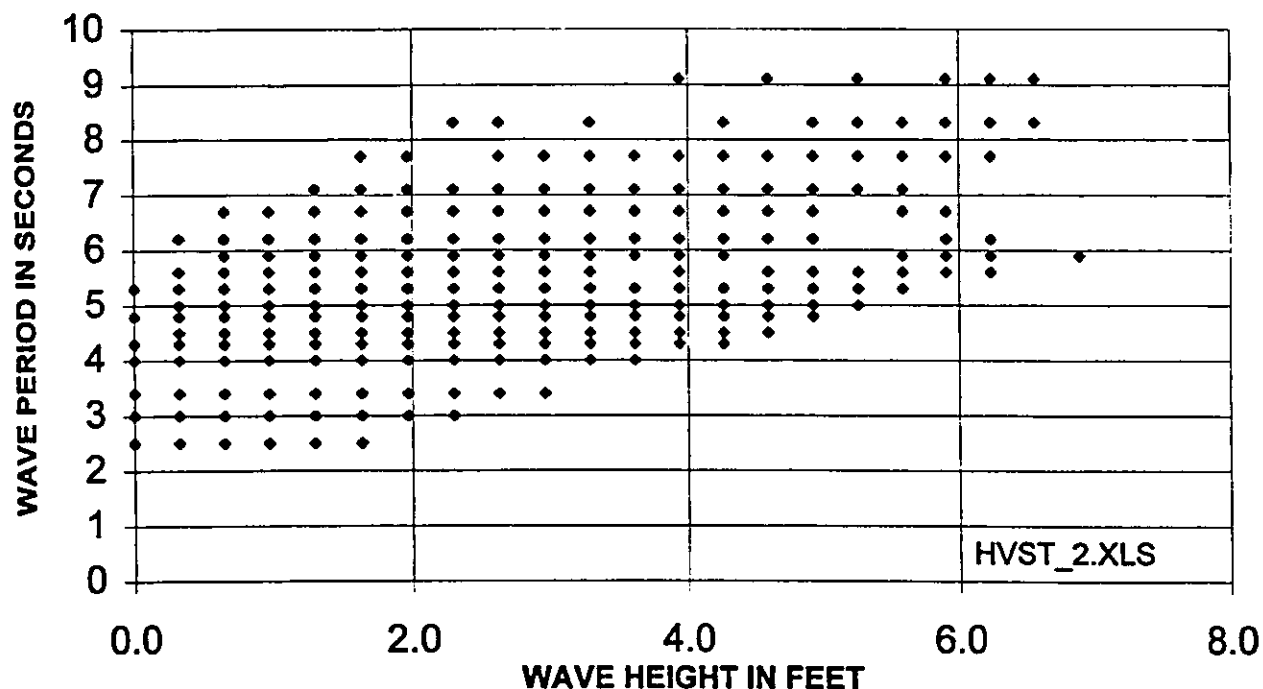


Figure 12. Typical Lakeside Dike Cross-Section for Proposed CDF

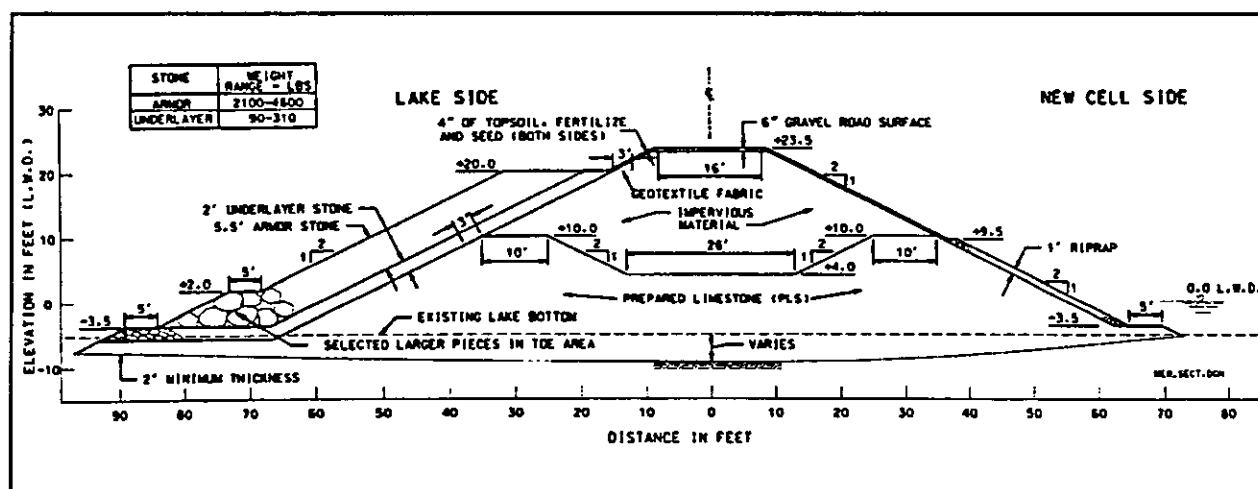


Figure 13. Potential CDF Locations Identified in Final EIS Dated June 1990

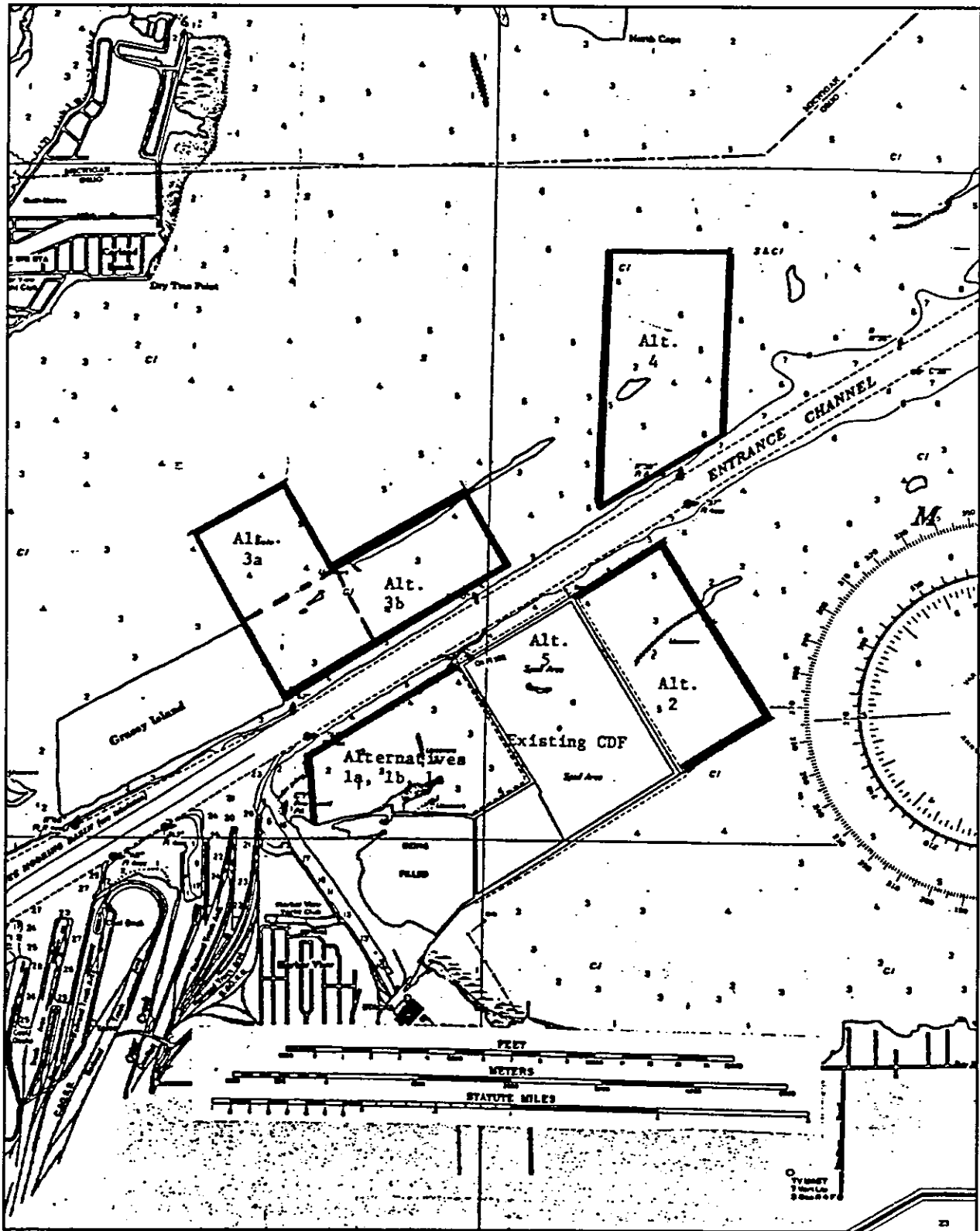


Figure 14. Depth Contours Used to Calculate Volume of Proposed CDF Adjacent to Cell 1 for Varying Widths

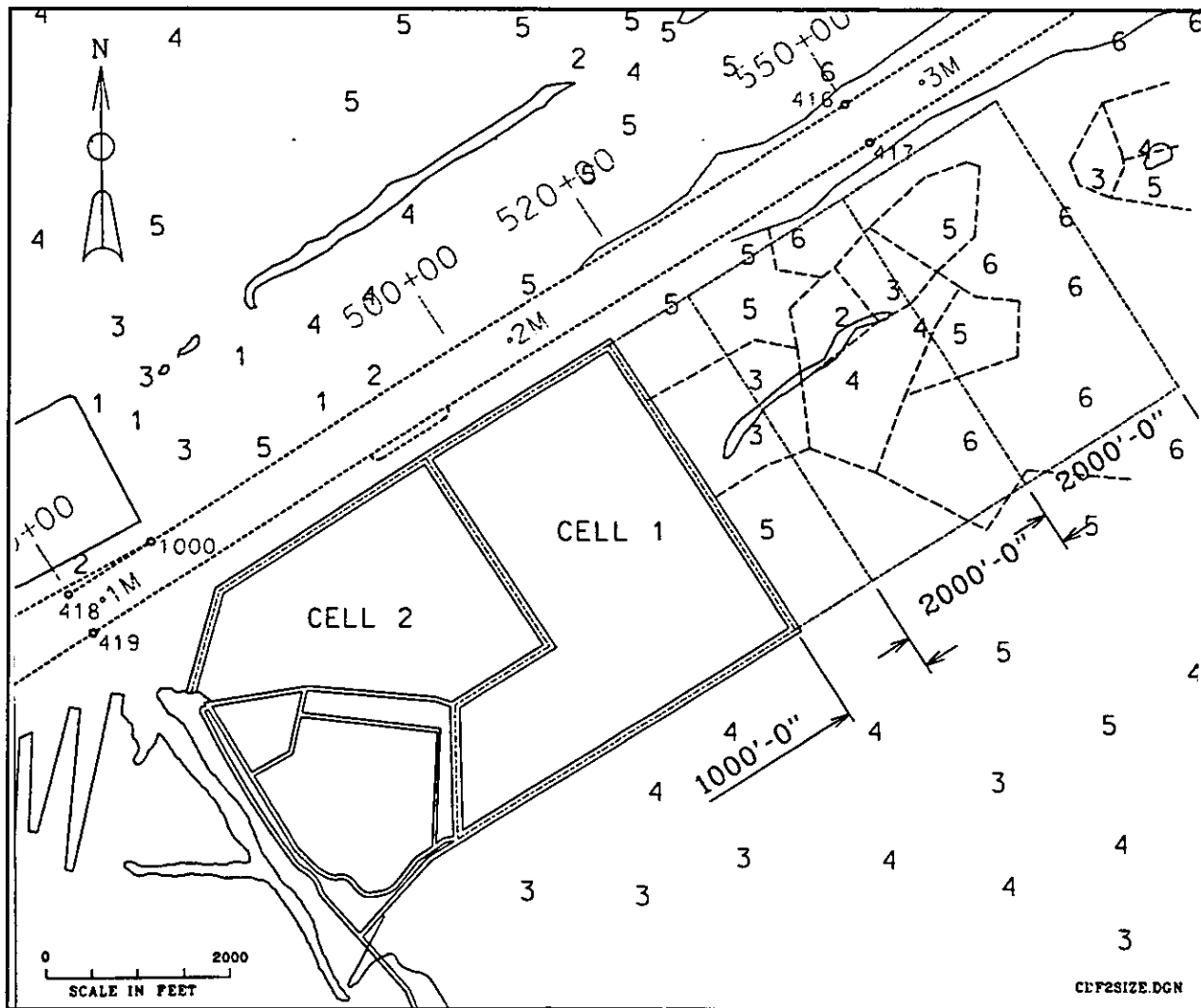


Figure 15. Dredged Storage Capacity of Proposed CDF Adjacent to Cell 1

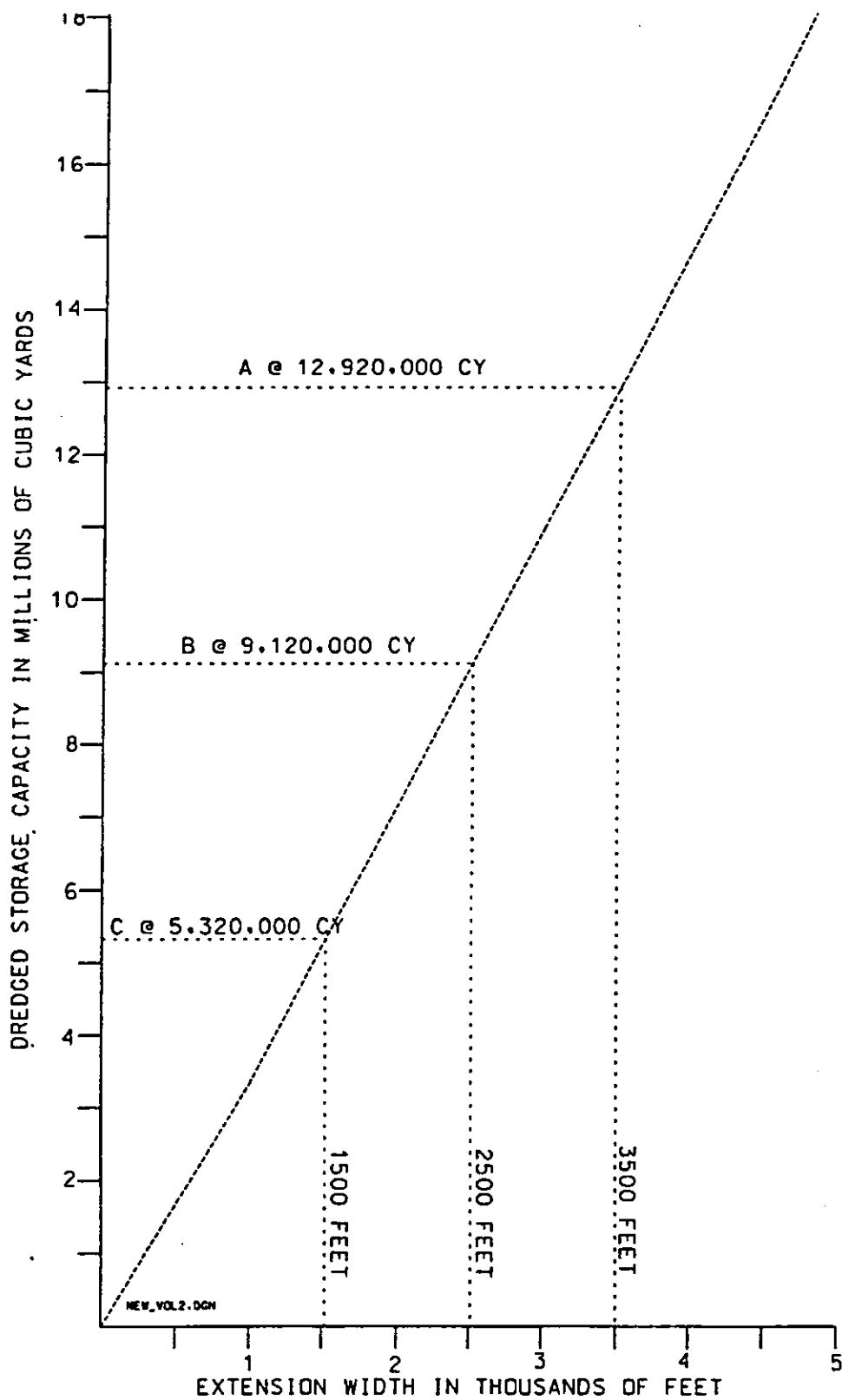


Figure 16. Proposed CDF Adjacent to Cell 1, Alternative Size A

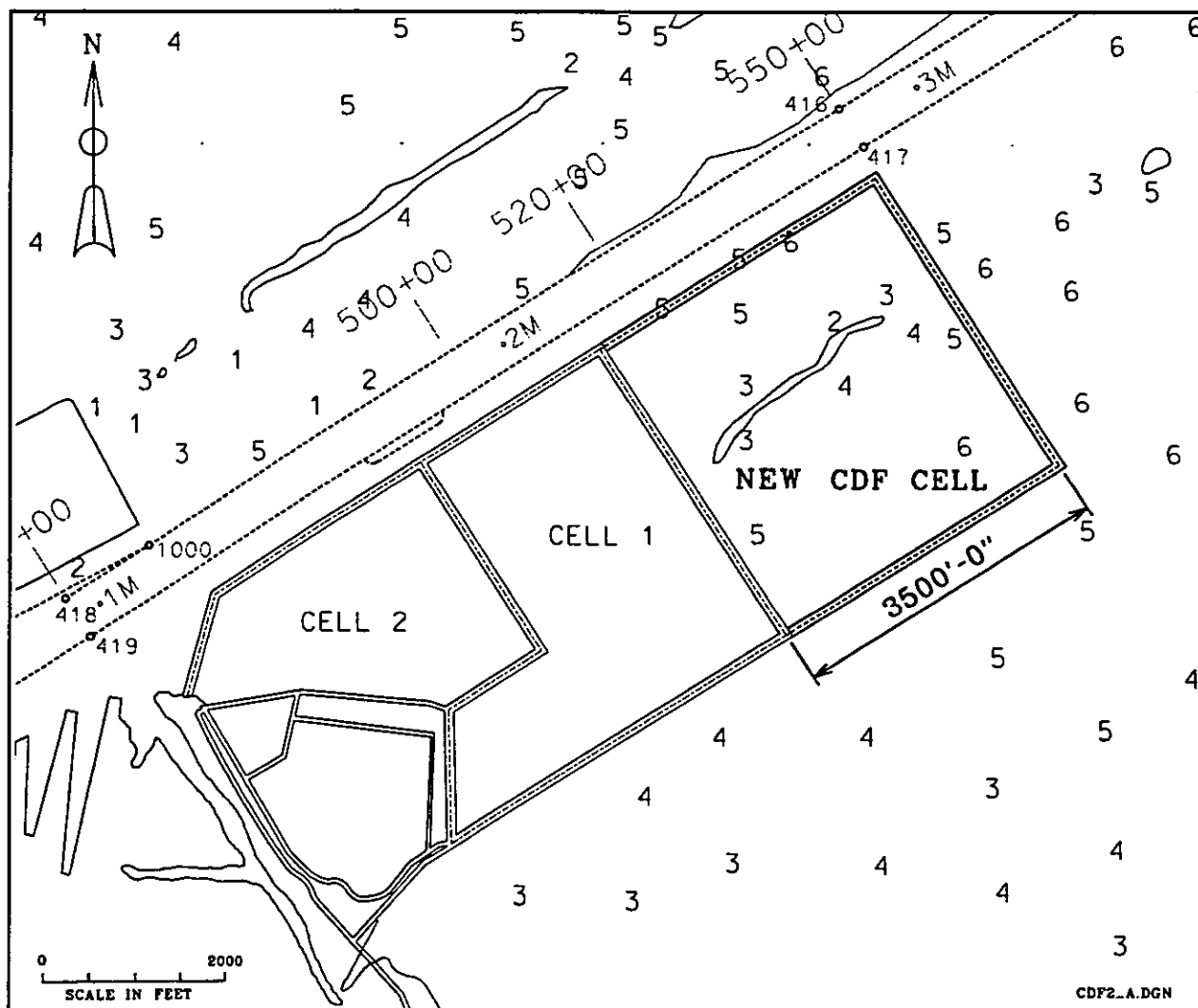


Figure 17. Proposed CDF Adjacent to Cell 1, Alternative Size B

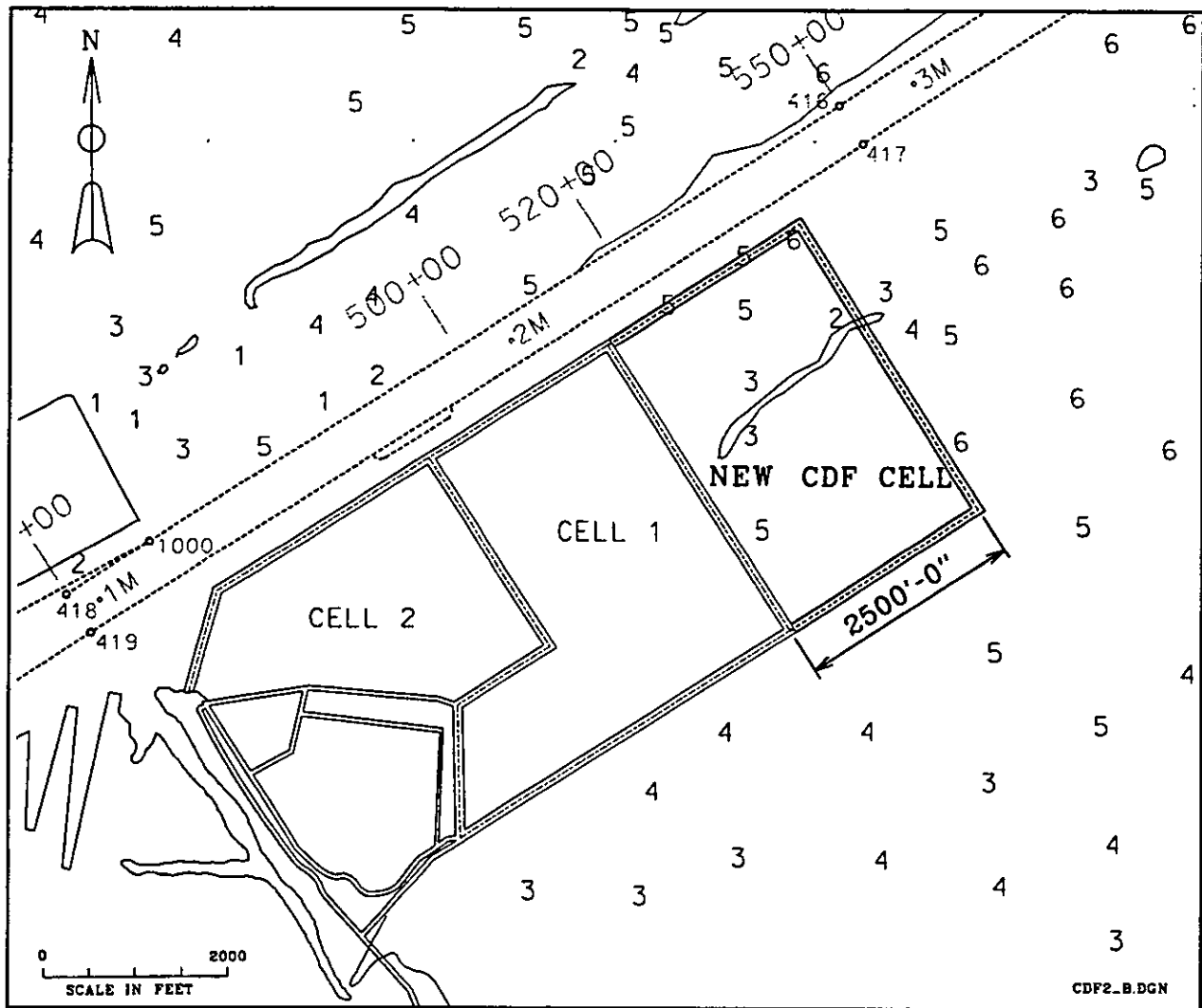
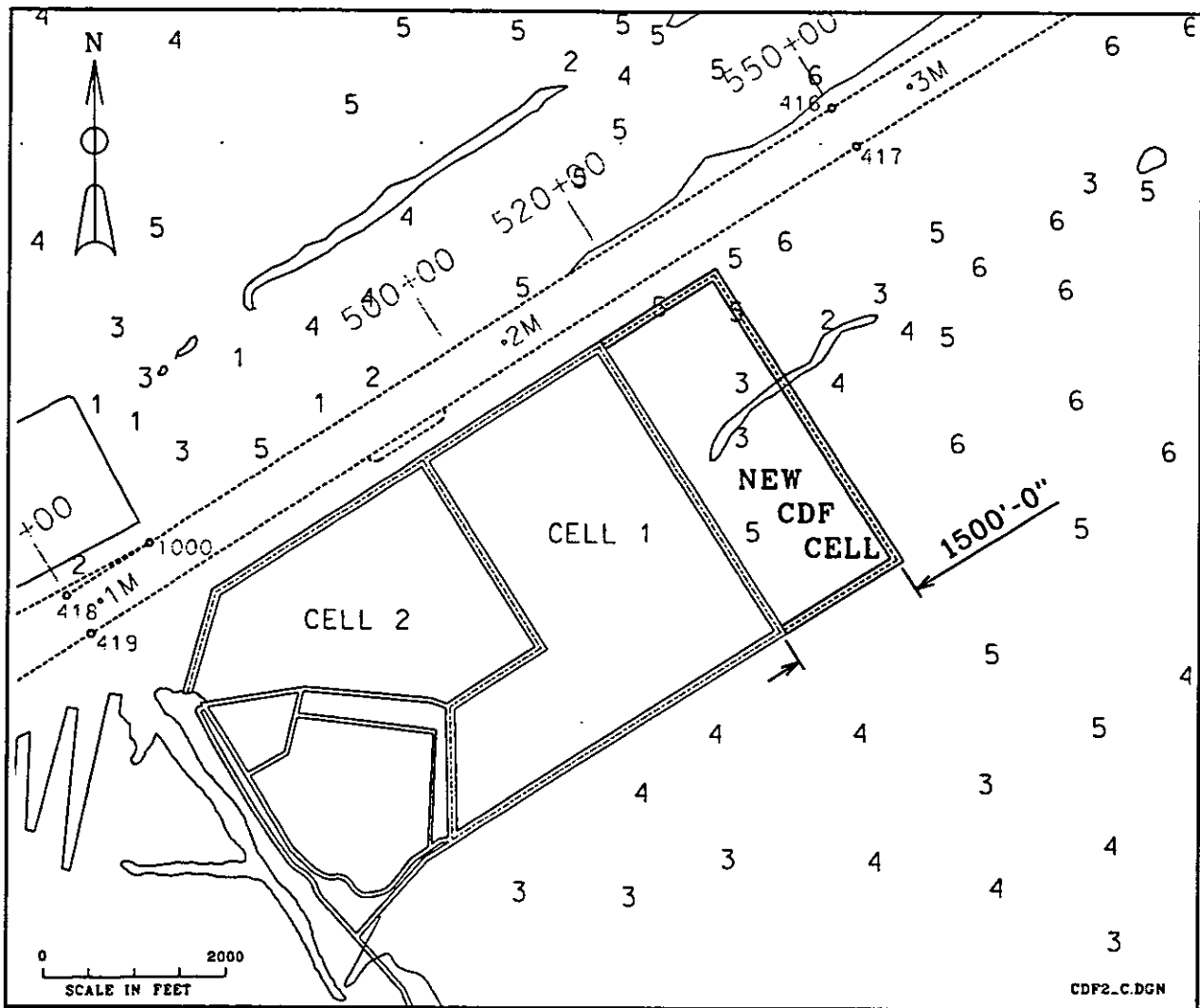


Figure 18. Proposed CDF Adjacent to Cell 1, Alternative Size C



**Figure 19. Depth Contours Used to Calculate Volume of Proposed CDF
Adjacent to Island 18, for Varying Widths**

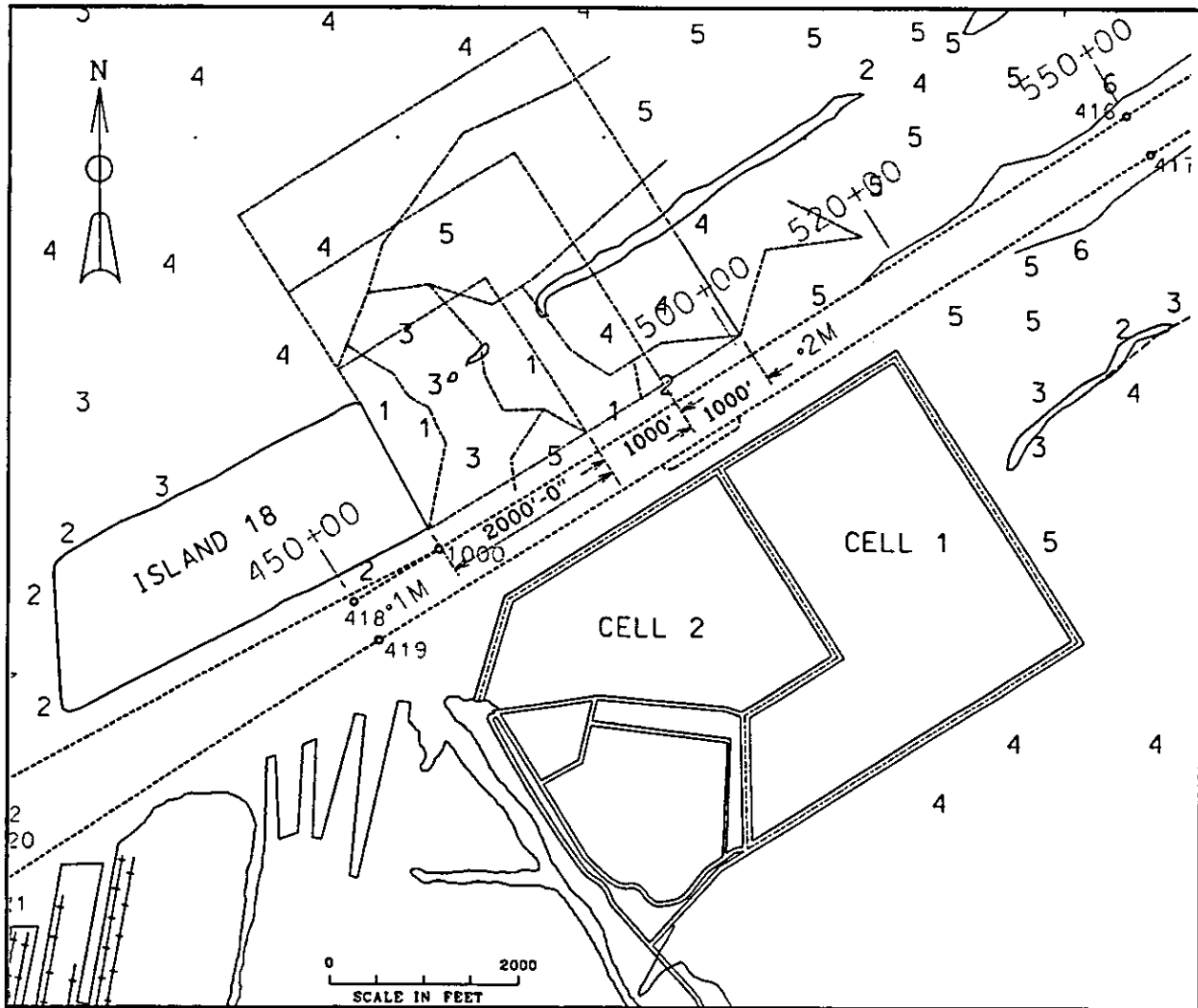


Figure 20. Dredged Storage Capacity of Proposed CDF Adjacent to Island 18

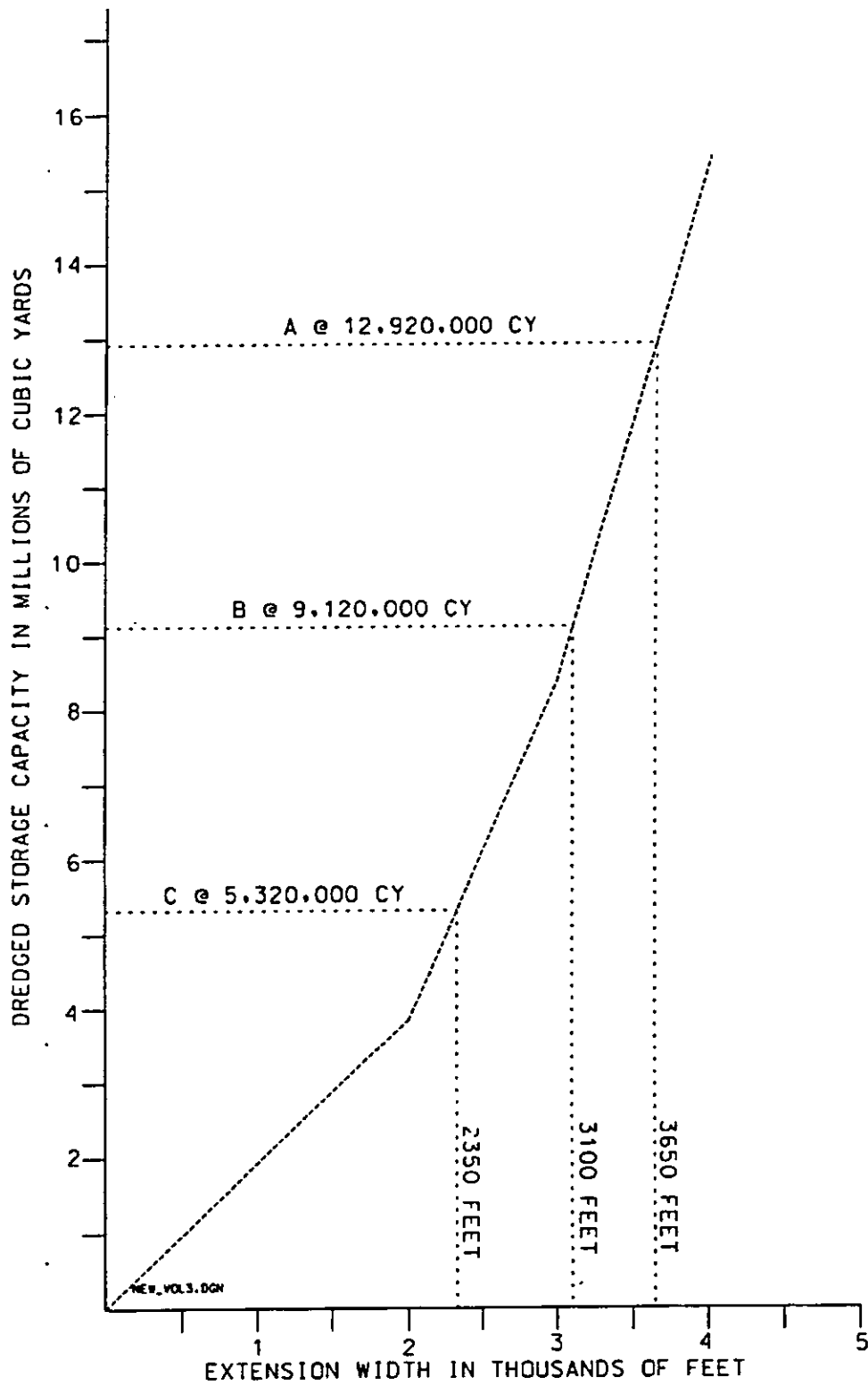


Figure 21. Proposed CDF Adjacent to Island 18, Alternative Size A

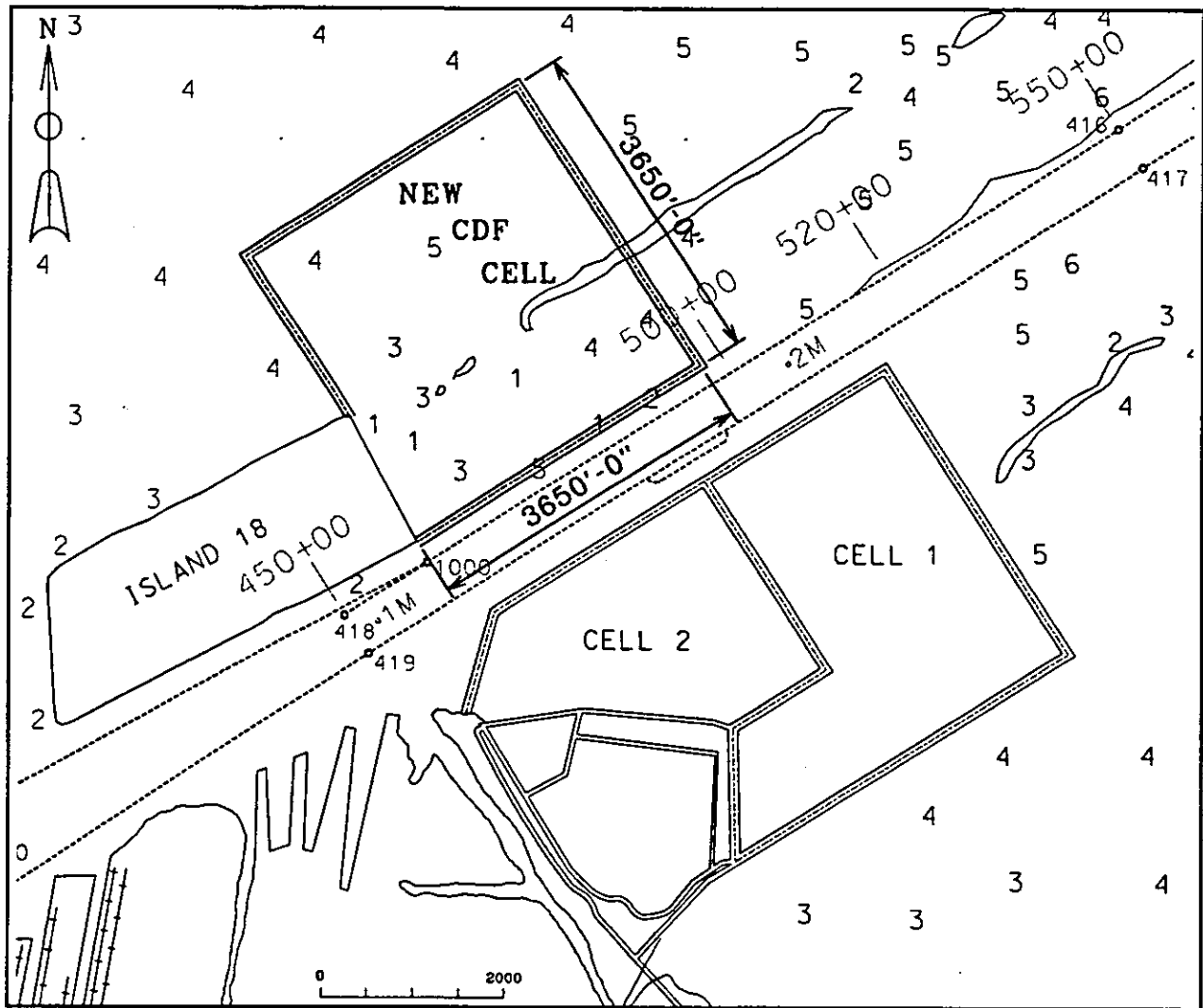


Figure 22. Proposed CDF Adjacent to Island 18, Alternative Size B

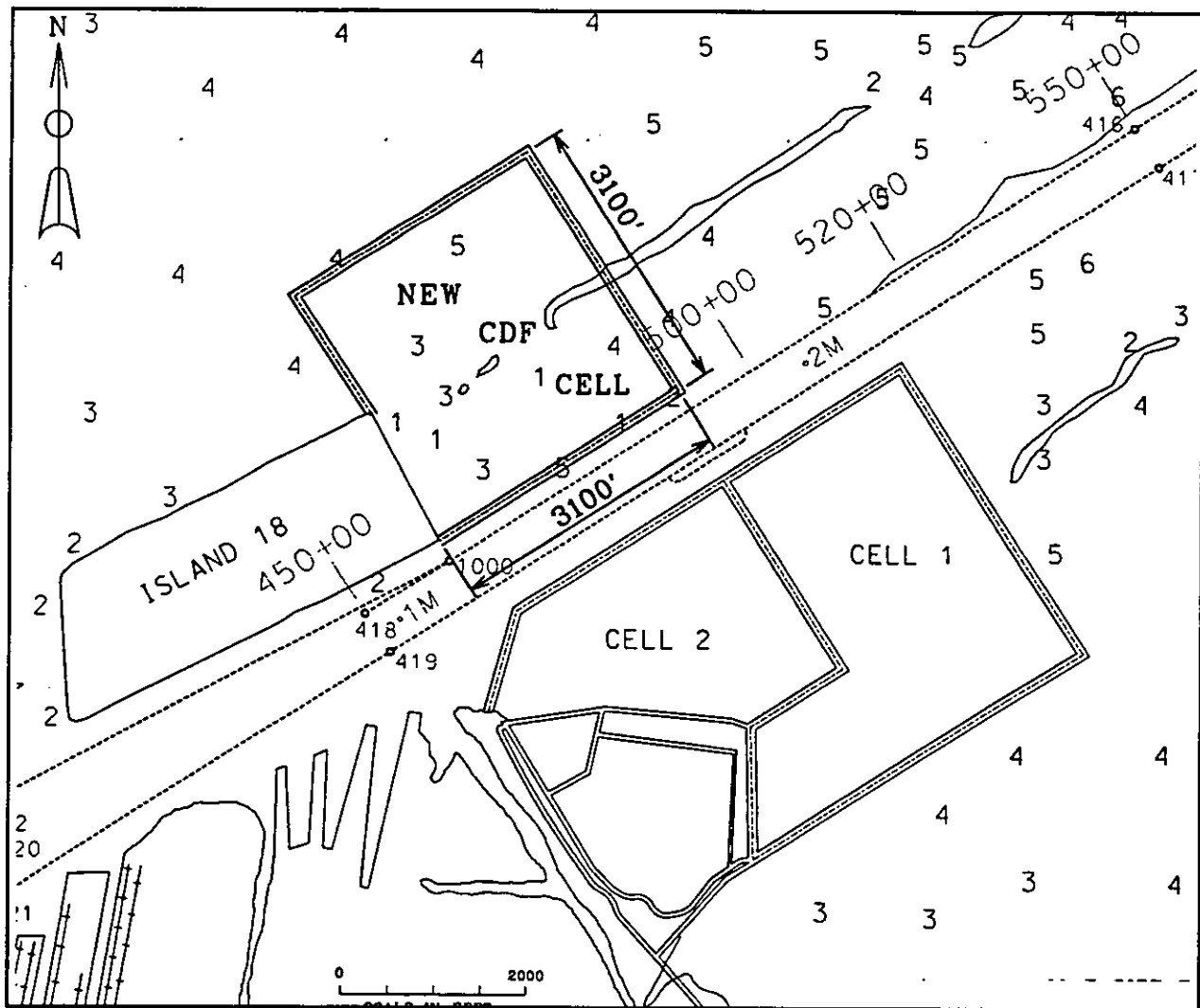


Figure 23. Proposed CDF Adjacent to Island 18, Alternative Size C

